

Dalitz Plot Analyses of $B^- \rightarrow D^+ \pi^- \pi^-$, $B^+ \rightarrow \pi^+ \pi^- \pi^+$ and $D_s^+ \rightarrow \pi^+ \pi^- \pi^+$ at *BABAR*

Liaoyuan Dong*†
 (On behalf of the *BABAR* Collaboration)
 Iowa State University, Ames, Iowa 50011-3160, USA

We report on the Dalitz plot analyses of $B^- \rightarrow D^+ \pi^- \pi^-$, $B^+ \rightarrow \pi^+ \pi^- \pi^+$ and $D_s^+ \rightarrow \pi^+ \pi^- \pi^+$. The Dalitz plot method and the most recent *BABAR* results are discussed.

1. Introduction

Dalitz plot analysis is an excellent way to study the dynamics of three-body decays. The decays under study are expected to proceed predominantly through intermediate quasi-two-body modes [1] and experimentally this is the observed pattern. Dalitz plot analysis can explore resonance properties, measure corresponding magnitudes and phases, and investigate corresponding *CP* asymmetries.

We report on the Dalitz plot analyses of $B^- \rightarrow D^+ \pi^- \pi^-$, $B^+ \rightarrow \pi^+ \pi^- \pi^+$ and $D_s^+ \rightarrow \pi^+ \pi^- \pi^+$. The data were collected with the *BABAR* detector at the PEP-II asymmetric-energy e^+e^- storage rings at SLAC. A detailed description of the *BABAR* detector is given in Ref. [2]. Monte Carlo (MC) simulation is used to study the detector response, its acceptance, background, and to validate the analysis.

2. Dalitz Plot Analysis

In the decay of a spin-0 particle A to a final state composed of three pseudo-scalar particles (abc), the differential decay rate is generally given in terms of the Lorentz-invariant matrix element \mathcal{M} by

$$\frac{d^2\Gamma}{dx dy} = \frac{|\mathcal{M}|^2}{256\pi^3 m_A^3}, \quad (1)$$

where m_A is the A particle mass, x and y are the invariant masses-squared of the ab and ac pairs, respectively. The Dalitz plot provides a graphical representation of the variation of the square of the matrix element, $|\mathcal{M}|^2$, over the kinematically accessible phase space (x,y) of the process.

The distribution of candidate events in the Dalitz plot is described in terms of a probability density function (PDF). The PDF is the sum of signal and back-

ground components and has the form:

$$\text{PDF}(x,y) = f_{\text{bg}} \frac{B(x,y)}{\int_{\text{DP}} B(x,y) dx dy} + (1 - f_{\text{bg}}) \frac{[S(x,y) \otimes \mathcal{R}] \epsilon(x,y)}{\int_{\text{DP}} [S(x,y) \otimes \mathcal{R}] \epsilon(x,y) dx dy}, \quad (2)$$

where

- The integral is performed over the whole Dalitz plot (DP).
- S ($= |\mathcal{M}|^2$) and B describe signal and background amplitude contributions, respectively.
- The $S(x,y) \otimes \mathcal{R}$ is the signal term convolved with the signal resolution function, the signal resolution can be safely neglected for broad resonances.
- f_{bg} is the fraction of background events.
- ϵ is the reconstruction efficiency.

An unbinned maximum likelihood fit to the Dalitz plot is performed in order to maximize the value of

$$\mathcal{L} = \prod_{i=1}^{N_{\text{event}}} \text{PDF}(x_i, y_i) \quad (3)$$

with respect to the parameters used to describe S , where x_i and y_i are the values of x and y for event i respectively, and N_{event} is the number of events in the Dalitz plot. In practice, the negative-log-likelihood (NLL) value

$$\text{NLL} = -\ln \mathcal{L} \quad (4)$$

is minimized in the fit.

The isobar model formulation is used, in which the signal decays are described by a coherent sum of a number of two-body amplitudes. The total decay matrix element \mathcal{M} is given by

$$\mathcal{M} = \sum_k \rho_k e^{i\phi_k} A_k, \quad (5)$$

*Email: dongly@ihep.ac.cn

†Current Address: Institute of High Energy Physics, Beijing 100049, China

where ρ_k and ϕ_k are the magnitudes and phases of the k^{th} decay mode respectively, the A_k distributions for resonant contribution describe the dynamics of the decay amplitudes and are written as the product of a relativistic Breit-Wigner function, two Blatt-Weisskopf barrier form factors [3] and an angular function [4].

The efficiency-corrected fraction due to the resonant or non-resonant contribution k is defined as follows:

$$f_k = \frac{|\rho_k|^2 \int_{\text{DP}} |A_k|^2 dx dy}{\int_{\text{DP}} |\mathcal{M}|^2 dx dy}. \quad (6)$$

The f_k values do not necessarily add to 1 because of interference effects. The uncertainty on each f_k is evaluated by propagating the full covariance matrix obtained from the fit.

3. Results from *BABAR*

3.1. $B^- \rightarrow D^+ \pi^- \pi^-$ [5]

We reconstruct the decays $B^- \rightarrow D^+ \pi^- \pi^-$ [6] with $D^+ \rightarrow K^- \pi^+ \pi^+$ based on a sample of about $383 \times 10^6 \Upsilon(4S) \rightarrow B\bar{B}$ decays. The resulting Dalitz plot distribution for data is shown in Fig. 1. The number of signal events in the Dalitz plot is 3414 ± 85 . The background fraction is about 30.4%. The background is parametrized using the MC simulation.

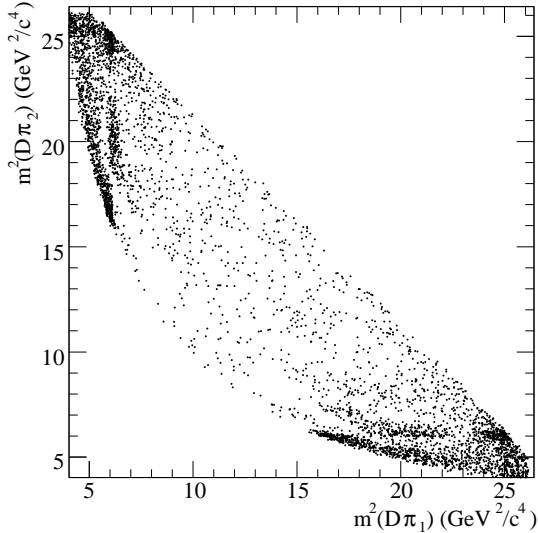


Figure 1: Dalitz plot for $B^- \rightarrow D^+ \pi^- \pi^-$.

The nominal fit model contains D_2^{*0} , D_0^{*0} , $D^*(2007)^0$, B^* and \mathcal{P} -wave non-resonant contributions. The \mathcal{S} -wave and \mathcal{D} -wave non-resonant contributions are found to be small and can be ignored. Replacing the $D^*(2007)^0$ by a $D\pi$ \mathcal{S} -wave [7] state is found to give a much worse fit.

Fig. 2a, 2b and 2c show the $m_{\text{min}}^2(D\pi)$, $m_{\text{max}}^2(D\pi)$ and $m^2(\pi\pi)$ projections respectively. Here $m_{\text{max}}^2(D\pi)$

and $m_{\text{min}}^2(D\pi)$ are the heavy and light invariant masses-squared of the $D\pi$ systems, respectively. The distributions in Fig. 2 show good agreement between the data and the fit.

We have performed some tests with the broad resonance D_0^{*0} excluded or with the J^P of the broad resonance replaced by other quantum numbers. In all cases, the NLL values are significantly worse than that of the nominal fit. We conclude that a broad spin-0 state D_0^{*0} is required in the fit to the data.

The total branching fraction of the $B^- \rightarrow D^+ \pi^- \pi^-$ decay is measured to be

$$\mathcal{B}(B^- \rightarrow D^+ \pi^- \pi^-) = (1.08 \pm 0.03 \pm 0.05) \times 10^{-3},$$

where the first error is statistical and the second is systematic. The systematic error on the measurement of the total $B^- \rightarrow D^+ \pi^- \pi^-$ branching fraction is due to the uncertainties on the number of $B^+ B^-$ events, the charged track reconstruction and identification efficiencies, the $D^+ \rightarrow K^- \pi^+ \pi^+$ branching fraction, the background shape and the fit models.

The mass and width of D_2^{*0} are determined to be:

$$\begin{aligned} m_{D_2^{*0}} &= (2460.4 \pm 1.2 \pm 1.2 \pm 1.9) \text{ MeV}/c^2 \text{ and} \\ \Gamma_{D_2^{*0}} &= (41.8 \pm 2.5 \pm 2.1 \pm 2.0) \text{ MeV}, \end{aligned}$$

respectively, while for the D_0^{*0} they are:

$$\begin{aligned} m_{D_0^{*0}} &= (2297 \pm 8 \pm 5 \pm 19) \text{ MeV}/c^2 \text{ and} \\ \Gamma_{D_0^{*0}} &= (273 \pm 12 \pm 17 \pm 45) \text{ MeV}, \end{aligned}$$

where the first and second errors reflect the statistical and systematic uncertainties, respectively, the third one is the uncertainty related to the fit models and the Blatt-Weisskopf barrier factors.

We have also obtained exclusive branching fractions for D_2^{*0} and D_0^{*0} production:

$$\begin{aligned} \mathcal{B}(B^- \rightarrow D_2^{*0} \pi^-) \times \mathcal{B}(D_2^{*0} \rightarrow D^+ \pi^-) \\ &= (3.5 \pm 0.2 \pm 0.2 \pm 0.4) \times 10^{-4} \text{ and} \\ \mathcal{B}(B^- \rightarrow D_0^{*0} \pi^-) \times \mathcal{B}(D_0^{*0} \rightarrow D^+ \pi^-) \\ &= (6.8 \pm 0.3 \pm 0.4 \pm 2.0) \times 10^{-4}. \end{aligned}$$

The relative phase of the scalar and tensor amplitude is measured to be

$$\phi_{D_0^{*0}} = -2.07 \pm 0.06 \pm 0.09 \pm 0.18 \text{ rad.}$$

The systematic uncertainties that affect the results of Dalitz plot analysis are due to the background parametrization, the selection criteria, and the possible fit bias.

Our results for the masses, widths and branching fractions are consistent with but more precise than previous measurements performed by Belle [8].

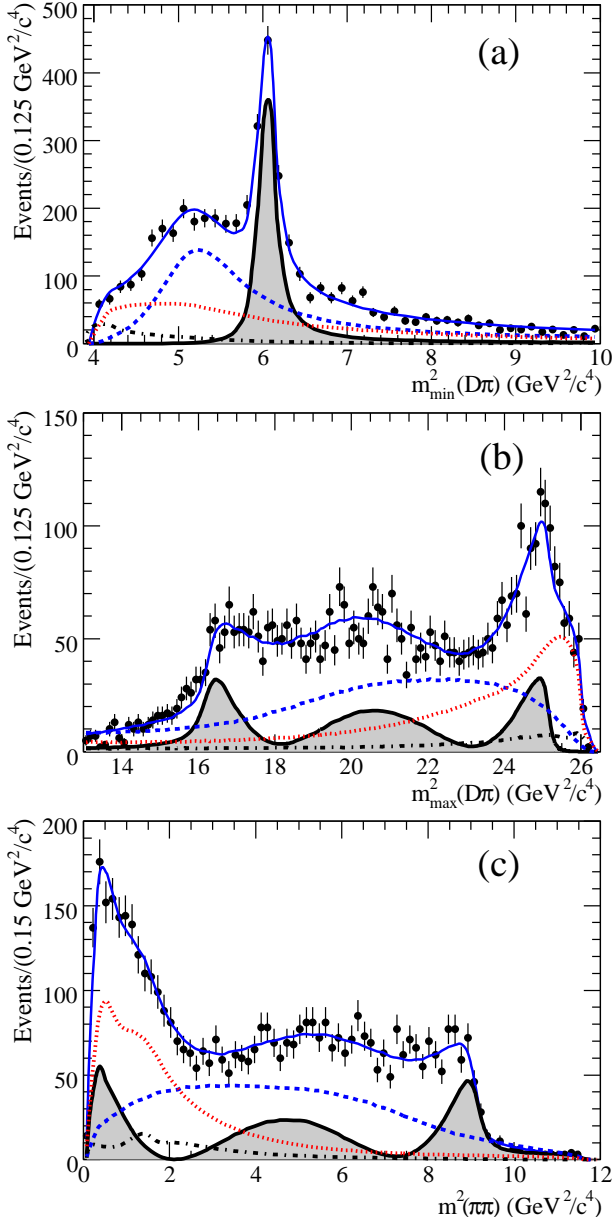


Figure 2: Result of the nominal fit to the data: projections on (a) $m_{\min}^2(D\pi)$, (b) $m_{\max}^2(D\pi)$ and (c) $m^2(\pi\pi)$. The points with error bars are data, the solid curves represent the nominal fit. The shaded areas show the D_2^{*0} contribution, the dashed curves show the D_0^{*0} signal, the dash-dotted curves show the $D^*(2007)^0$ and B^* signals, and the dotted curves show the background.

3.2. $B^+ \rightarrow \pi^+\pi^-\pi^+$ [9]

We fit the B^- and B^+ samples independently in order to determine the CP asymmetry. The total signal amplitudes for B^+ and B^- decays are given by

$$\mathcal{M} = \sum_j c_j A_j(m_{\max}^2, m_{\min}^2),$$

$$\bar{\mathcal{M}} = \sum_j \bar{c}_j \bar{A}_j(m_{\max}^2, m_{\min}^2), \quad (7)$$

where m_{\max}^2 and m_{\min}^2 are the heavy and light invariant masses-squared of the $\pi^\pm\pi^\mp$ systems, respectively. The complex coefficients c_j and \bar{c}_j for a given decay mode j contain all the weak phase dependence. Since the A_j terms contain only strong dynamics, $A_j \equiv \bar{A}_j$. The CP asymmetry for each contributing resonance is determined from the fitted parameters

$$\mathcal{A}_{CP,j} = \frac{|\bar{c}_j|^2 - |c_j|^2}{|\bar{c}_j|^2 + |c_j|^2}. \quad (8)$$

We reconstruct the decays $B^+ \rightarrow \pi^+\pi^-\pi^+$ based on a sample of about $465 \times 10^6 \Upsilon(4S) \rightarrow B\bar{B}$ decays. We reject background from two-body decays of D^0 meson and charmonium states (J/ψ and $\psi(2S)$) by excluding invariant masses (in units of GeV/c^2) in the ranges: $1.660 < m_{\pi^+\pi^-} < 1.920$, $3.051 < m_{\pi^+\pi^-} < 3.222$, and $3.660 < m_{\pi^+\pi^-} < 3.820$. The background-subtracted Dalitz plot distribution for data is shown in Fig. 3. We fit 4335 B candidates to calculate the fit fractions and CP asymmetries. The background is parametrized using the MC simulation.

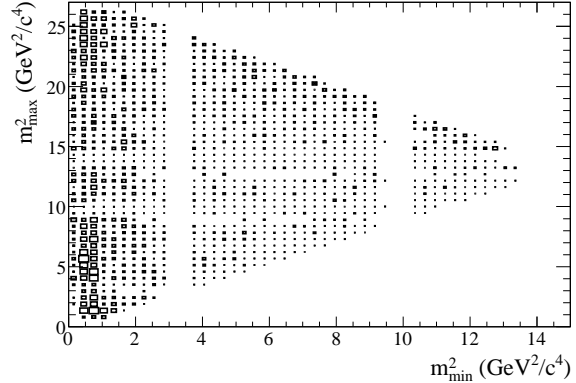


Figure 3: Background-subtracted Dalitz plot for $B^+ \rightarrow \pi^+\pi^-\pi^+$. The plot shows bins with greater than zero entries. The depleted bands are the charm and charmonia exclusion regions.

The nominal signal Dalitz plot model comprises a momentum-dependent non-resonant component and four intermediate resonance states: $\rho^0(770)\pi^\pm$, $\rho^0(1450)\pi^\pm$, $f_2(1270)\pi^\pm$, and $f_0(1370)\pi^\pm$. We do not find any significant contributions from $f_0(980)\pi^\pm$, $\chi_{c0}\pi^\pm$, or $\chi_{c2}\pi^\pm$. The absence of the charmonium contributions precludes the extraction of the unitarity triangle angle γ . We find no evidence for direct CP violation. The inclusive CP asymmetry is determined to be $(+3.2 \pm 4.4 \pm 3.1_{-2.0}^{+2.5})\%$, where the uncertainties are statistical, systematic, and model-dependent, respectively.

Projections of the data, with the fit result overlaid, as $\pi^\pm\pi^\mp$ invariant-mass distributions can be seen in

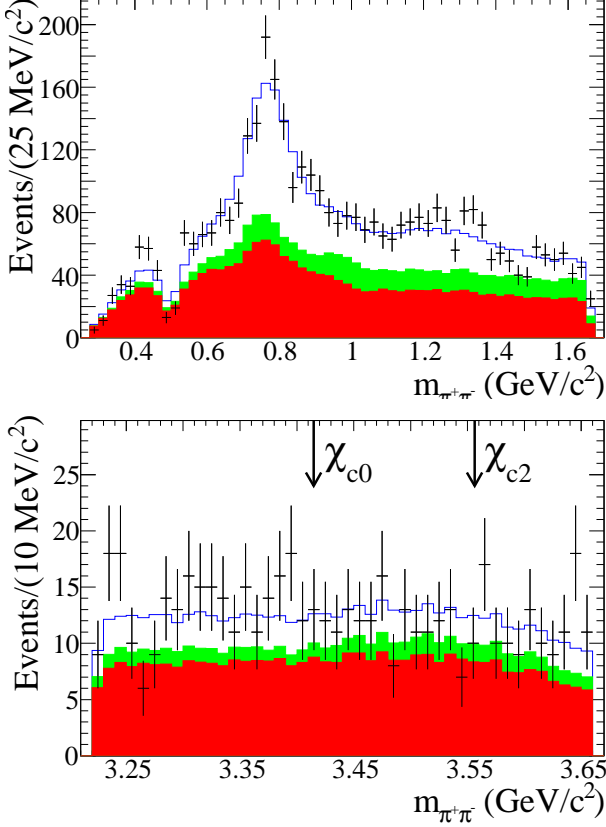


Figure 4: Dipion invariant mass projections: (upper) in the $\rho^0(770)$ region; and (lower) in the regions of χ_{c0} and χ_{c2} . The data are the points with statistical error bars, the dark-shaded (red) histogram is the $q\bar{q}$ component, the light-shaded (green) histogram is the $B\bar{B}$ background contribution, while the upper (blue) histogram shows the total fit result. The dip near $0.5 \text{ GeV}/c^2$ in the upper plot is due to the rejection of events containing K_s^0 candidates.

Fig.4. The agreement between the fit results and the data is generally good.

The Dalitz plot is dominated by the $\rho^0(770)$ resonance and a non-resonant contribution. The mass and width of the $f_0(1370)$ are determined to be $m_{f_0(1370)} = 1400 \pm 40 \text{ MeV}/c^2$ and $\Gamma_{f_0(1370)} = 300 \pm 80 \text{ MeV}$ (statistical uncertainties only). We measure the branching fractions $\mathcal{B}(B^\pm \rightarrow \pi^\pm \pi^\pm \pi^\mp) = (15.2 \pm 0.6 \pm 1.2 \pm 0.4) \times 10^{-6}$, $\mathcal{B}(B^\pm \rightarrow \rho^0(770)\pi^\pm) = (8.1 \pm 0.7 \pm 1.2^{+0.4}_{-1.1}) \times 10^{-6}$, $\mathcal{B}(B^\pm \rightarrow f_2(1270)\pi^\pm) = (1.57 \pm 0.42 \pm 0.16^{+0.53}_{-0.19}) \times 10^{-6}$, and $\mathcal{B}(B^\pm \rightarrow \pi^\pm \pi^\pm \pi^\mp \text{ non-resonant}) = (5.3 \pm 0.7 \pm 0.6^{+1.1}_{-0.5}) \times 10^{-6}$, where the uncertainties are statistical, systematic, and model-dependent, respectively. We have made the first observation of the decay $B^\pm \rightarrow f_2(1270)\pi^\pm$ with a statistical significance of 6.1σ .

The systematic uncertainties that affect the results of Dalitz plot analysis are due to the the number of B^+B^- events, signal and background PDF

parametrization, the charged track reconstruction and identification efficiencies, and the possible fit bias.

Our results will be useful to reduce model uncertainties in the extraction of the CKM angle α from time-dependent Dalitz plot analysis of $B^0 \rightarrow \pi^+\pi^-\pi^0$.

3.3. $D_s^+ \rightarrow \pi^+\pi^-\pi^+$ [10]

We reconstruct $D_s^+ \rightarrow \pi^+\pi^-\pi^+$ based on 384 fb^{-1} data sample. We use the tag of $D_s^{*(2112)^+} \rightarrow D_s^+\gamma$ to reduce the combinatorial background. The signal PDFs are build using the $D_s^+ \rightarrow K^+K^-\pi^+$. The reconstructed D_s^+ sample contains 13179 events with a purity of 80%. The background shape is obtained by fitting the D_s^+ sidebands. The Dalitz plot distribution for data is shown in Fig. 5.

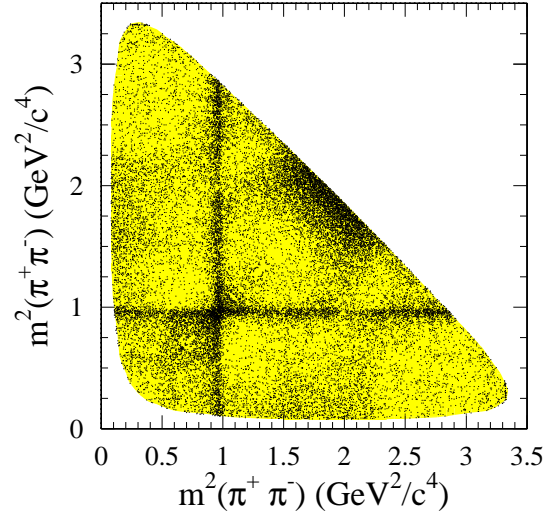


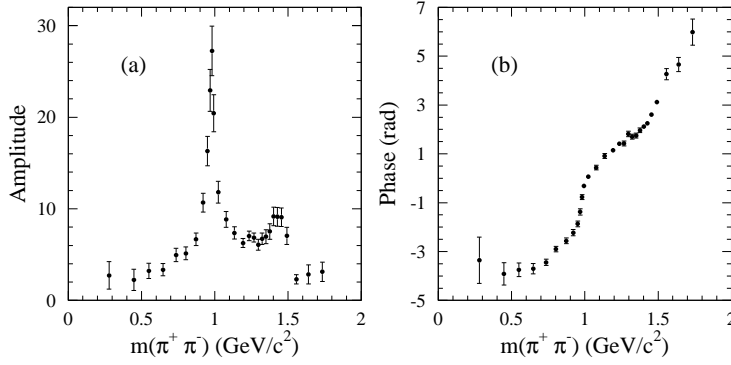
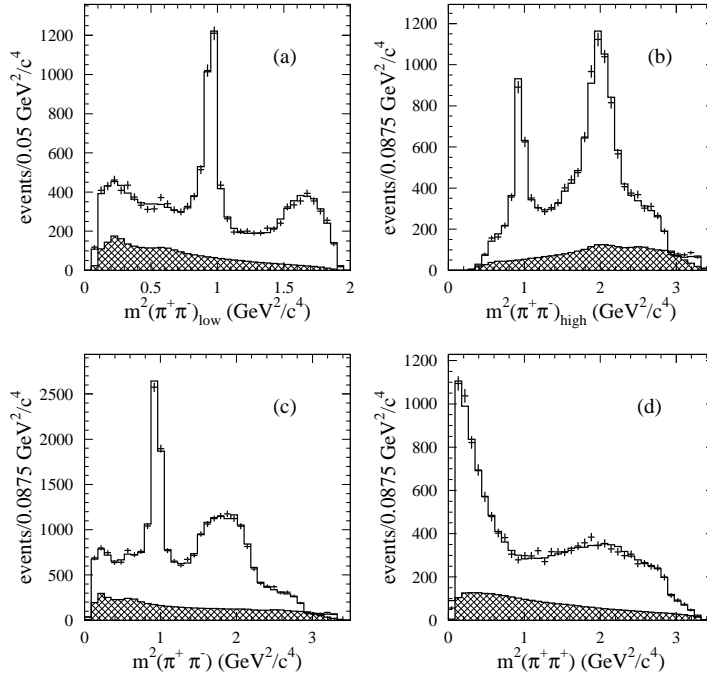
Figure 5: Dalitz plot for $D_s^+ \rightarrow \pi^+\pi^-\pi^+$.

For the $\pi^+\pi^-$ \mathcal{S} -wave amplitude, we use a model-independent partial wave analysis: instead of including the \mathcal{S} -wave amplitude as a superposition of relativistic Breit-Wigner functions, we divide the $\pi^+\pi^-$ mass spectrum into 29 slices and we parametrize the \mathcal{S} -wave by an interpolation between the 30 endpoints in the complex plane:

$$A_{\mathcal{S}\text{-wave}}(m_{\pi\pi}) = \text{Interp}(c_k(m_{\pi\pi})e^{i\phi_k(m_{\pi\pi}))_{k=1,\dots,30}}. \quad (9)$$

The amplitude and phase of each endpoint are free parameters. The width of each slice is tuned to get approximately the same number of $\pi^+\pi^-$ combinations ($\approx 13179 \times 2/29$). Interpolation is implemented by a Relaxed Cubic Spline [11]. The phase is not constrained in a specific range in order to allow the spline to be a continuous function.

The nominal signal Dalitz plot model includes $f_2(1270)$, $\rho(770)$, $\rho(1450)$ and $\pi\pi$ \mathcal{S} -wave. The Dalitz


 Figure 6: (a) \mathcal{S} -wave amplitude extracted from the best fit, (b) corresponding \mathcal{S} -wave phase.

 Figure 7: Dalitz plot projections (points with error bars) and fit results (solid histogram). (a) $m^2(\pi^+\pi^-)_{\text{low}}$, (b) $m^2(\pi^+\pi^-)_{\text{high}}$, (c) total $m^2(\pi^+\pi^-)$, (d) $m^2(\pi^+\pi^+)$. The hatched histograms show the background distribution.

plot is dominated by the $D_s \rightarrow (\pi^+\pi^-)_{\mathcal{S}\text{-wave}}\pi^+$ contribution. The \mathcal{S} -wave shows, in both amplitude and phase, the expected behavior for the $f_0(980)$ resonance, and further activity in the regions of the $f_0(1370)$ and $f_0(1500)$ resonances. The \mathcal{S} -wave is small in the $f_0(600)$ region, indicating that this resonance has a small coupling to $s\bar{s}$.

The resulting \mathcal{S} -wave $\pi^+\pi^-$ amplitude and phase is shown in Fig. 6a and 6b. Our results on the amplitude and phase of the $\pi^+\pi^-$ \mathcal{S} -wave agree better (within uncertainties) with the results from FOCUS [12] than those from E791 [13]. The Dalitz plot projections together with the fit results are shown in Fig. 7.

Since $D_s^+ \rightarrow \pi^+\pi^-\pi^+$ and $D_s^+ \rightarrow K^+K^-\pi^+$ have similar topologies, the ratio of branching fractions is expected to have a reduced systematic uncertainty. We therefore select events from the two D_s decay modes using similar selection criteria for the D_s^{*+} selection. The ratio of branching fractions is evaluated as:

$$\frac{\mathcal{B}(D_s^+ \rightarrow \pi^+\pi^-\pi^+)}{\mathcal{B}(D_s^+ \rightarrow K^+K^-\pi^+)} = 0.199 \pm 0.004 \pm 0.009,$$

where the first error is statistical and the second is systematic. The systematic uncertainty comes from the MC statistics and from the selection criteria used.

4. Conclusion

We reviewed the recent results from the Dalitz plot analyses of $B^- \rightarrow D^+\pi^-\pi^-$, $B^+ \rightarrow \pi^+\pi^-\pi^+$ and $D_s^+ \rightarrow \pi^+\pi^-\pi^+$ performed by the BABAR Collaboration. The results can be summarized as follows:

- $B^- \rightarrow D^+\pi^-\pi^-$
We find the total branching fraction of the three-body decay: $\mathcal{B}(B^- \rightarrow D^+\pi^-\pi^-) = (1.08 \pm 0.03 \pm 0.05) \times 10^{-3}$. We observe the established D_2^{*0} and confirm the existence of D_0^{*0} in their decays to $D^+\pi^-$, we measure the masses and widths of D_2^{*0} and D_0^{*0} to be: $m_{D_2^{*0}} = (2460.4 \pm 1.2 \pm 1.2 \pm 1.9) \text{ MeV}/c^2$, $\Gamma_{D_2^{*0}} = (41.8 \pm 2.5 \pm 2.1 \pm 2.0) \text{ MeV}$, $m_{D_0^{*0}} = (2297 \pm 8 \pm 5 \pm 19) \text{ MeV}/c^2$ and $\Gamma_{D_0^{*0}} = (273 \pm 12 \pm 17 \pm 45) \text{ MeV}$.
- $B^+ \rightarrow \pi^+\pi^-\pi^+$
We measure the branching fractions $\mathcal{B}(B^\pm \rightarrow \pi^\pm\pi^\pm\pi^\mp) = (15.2 \pm 0.6 \pm 1.2 \pm 0.4) \times 10^{-6}$, $\mathcal{B}(B^\pm \rightarrow \rho^0(770)\pi^\pm) = (8.1 \pm 0.7 \pm 1.2^{+0.4}_{-1.1}) \times 10^{-6}$, $\mathcal{B}(B^\pm \rightarrow f_2(1270)\pi^\pm) = (1.57 \pm 0.42 \pm 0.16^{+0.53}_{-0.19}) \times 10^{-6}$, and $\mathcal{B}(B^\pm \rightarrow \pi^\pm\pi^\pm\pi^\mp \text{ non-resonant}) = (5.3 \pm 0.7 \pm 0.6^{+1.1}_{-0.5}) \times 10^{-6}$. We observe no significant direct CP asymmetries for the above modes, and there is no evidence for the decays $B^\pm \rightarrow f_0(980)\pi^\pm$, $B^\pm \rightarrow \chi_{c0}\pi^\pm$, or $B^\pm \rightarrow \chi_{c2}\pi^\pm$.
- $D_s^+ \rightarrow \pi^+\pi^-\pi^+$
We perform a high precision measurement of the ratio of branching fractions: $\mathcal{B}(D_s \rightarrow \pi^+\pi^-\pi^+)/\mathcal{B}(D_s \rightarrow K^+K^-\pi^+) = 0.199 \pm 0.004 \pm 0.009$. The amplitude and phase of

the $\pi^+\pi^-$ S -wave is extracted in a model-independent way for the first time.

References

- [1] M. Bauer, B. Stech, and M. Wirbel, Z. Phys. C **34**, 103 (1987).
- [2] B. Aubert *et al.*, [BABAR Collaboration], Nucl. Instrum. Methods A **479**, 1 (2002).
- [3] J. Blatt and V. Weisskopf, Theoretical Nuclear Physics, p.361, New York, John Wiley & Sons (1952).
- [4] C. Zemach, Phys. Rev. **140**, B97 (1965).
- [5] B. Aubert *et al.* [BABAR Collaboration], Phys. Rev. D **79**, 112004 (2009).
- [6] Charged conjugate states are implied throughout the paper.
- [7] D. V. Bugg, J. Phys. G **36**, 075003 (2009).
- [8] K. Abe *et al.*, [Belle Collaboration], Phys. Rev. D **69**, 112002 (2004).
- [9] B. Aubert *et al.* [BABAR Collaboration], Phys. Rev. D **79**, 072006 (2009).
- [10] B. Aubert *et al.* [BABAR Collaboration], Phys. Rev. D **79**, 032003 (2009).
- [11] K. S. Kölbig and H. Lipps, Cubic Splines and Their Integrals, CERN Program Library, E211.
- [12] J. M. Link *et al.* [FOCUS Collaboration], Phys. Lett. B **585**, 200 (2004).
- [13] E. M. Aitala *et al.* [E791 Collaboration], Phys. Rev. Lett. **86**, 765 (2001).

